

## Radiation properties of gamma-ray compact steep-spectrum sources

Shen-Shi Du<sup>1</sup>, Hai-Ming Zhang<sup>2</sup>, Ting-Feng Yi<sup>3</sup>, Jin Zhang<sup>4,\*</sup>, En-Wei Liang<sup>1</sup>

<sup>1</sup>*Guangxi Key Laboratory for Relativistic Astrophysics, Department of Physics, Guangxi University, Nanning 530004, China*

<sup>2</sup>*School of Astronomy and Space Science, Nanjing University, Nanjing 210023, China*

<sup>3</sup>*Department of Physics, Yunnan Normal University, Kunming 650500, China*

<sup>4</sup>*National Astronomical Observatories, Chinese Academy of Sciences, Beijing 100012, China; jinzhang@bao.ac.cn*

**Abstract** Three compact steep-spectrum sources (CSSs) have been detected by the *Fermi*/LAT. We collected their broadband SEDs from the literature and compared with two typical blazars, one BL Lacertae (BL Lac) and one flat spectrum radio quasar (FSRQ). The morphology of the broadband SEDs for the three CSSs is more analogous to FSRQs than BL Lacs. However, the multiband spectrum fitting may offer a complementary diagnostic clue of their gamma-ray emission production mechanisms and jet properties.

**Keywords:** Galaxies: Active, Galaxies: Jets, Radio Continuum: Galaxies, Gamma Rays: Galaxies

### 1. Introduction

So far, most confirmed extragalactic gamma-ray emission sources are blazars (Ackermann et al. 2015), for which the broadband spectral energy distributions (SEDs) are dominated by the jet emission and the jet direction points to the Earth. Blazars are divided into BL Lacertae (BL Lac) objects and flat spectrum radio quasars (FSRQs) according to their spectral features in the optical band. Generally, the observed SEDs of blazars are bimodal and can be well explained by the one-zone leptonic models; the synchrotron radiation and the inverse Compton (IC) scattering of relativistic electrons in the jets (Maraschi et al. 1992; Ghisellini et al. 1996; Sikora et al. 2009; Zhang et al. 2012, 2014, 2015).

Besides blazars, some other kinds of active galactic nuclei (AGNs) have also been detected by the *Fermi*/LAT, such as radio galaxies (RGs) and narrow-line Seyfert 1 (NLS1) galaxies (Ackermann et al. 2015). For both of them, the detected gamma-ray emission is also thought to be from the jet radiation. The SEDs of the GeV NLS1s are similar to blazars and can be well represented with the one-zone leptonic model. The jet properties of the GeV NLS1 galaxies are intermediate between FSRQ jets and BL Lac jets, but more analogous to FSRQ jets (Sun et al. 2015). According to the unification models for radio loud (RL) AGNs, BL Lacs are associated with FR I RGs, whereas FSRQs are usually linked with FR II RGs (Urry & Padovani 1995), i.e., RGs are the parent populations of blazars with large viewing angles and small Doppler factors. Although a more complex model with more parameters may produce a better fit to the

SEDs of some RGs (e.g., Tavecchio & Ghisellini 2014), the one-zone leptonic model is also used to reproduce the SEDs of RGs by many authors (Abdo et al. 2009a; Migliori et al. 2011; Fukazawa et al. 2015; Xue et al. 2017).

Another class of RL AGN, known as compact steep-spectrum sources (CSSs), is also detected in the GeV band by *Fermi*/LAT. The radio morphology of CSSs is typically characterized by fully developed radio lobes and by a small linear size ( $< 15$  kpc; see O’Dea 1998 for a review). CSS is thought to be the first stage in the evolution of large extragalactic radio sources (e.g., Migliori et al. 2014). The radiation mechanisms and origin of the gamma-ray emission are useful to study many aspects of the physics of CSSs. Comparisons of broadband emission between CSSs with blazars may help to reveal the intrinsic connections among different RL AGNs.

## 2. The gamma-ray Emission CSSs

**3C 286** also named B1328+307, at redshift of  $z = 0.849$  (Cohen et al. 1977). The steep radio spectrum with a spectral index of  $\alpha = -0.61$  ( $S_\nu \propto \nu^\alpha$ ) between 1.4 and 50 GHz with a turnover at about 300 MHz, below which it is flat till  $\sim 75$  MHz (An et al. 2017). The source displays a primary core and a second lobe  $\sim 2.6$  arcsec (19.4 kpc) to the south-west (Spencer et al. 1989; An et al. 2017). The radio emission at 15 GHz of this source is rather stable and no significant variation is observed in the past 10 years. The high polarization of the source has been detected in the radio band (Akujor & Garrington 1995). A compact bright nucleus associated with the radio core is also detected by the Hubble Space Telescope (deVries et al. 1997). Two compact components in the inner 10-mas region with comparable flux densities are resolved with the Very Long Baseline Interferometry (VLBI) and the more compact component showing an inverted spectrum with a turnover between 5 and 8 GHz may infer the core (An et al. 2017). A jet speed of  $\sim 0.5c$  and an inclination angle of  $\sim 48^\circ$  are derived for 3C 286. The optical spectrum observed with the SDSS-BOSS clearly indicates that 3C 286 can be classified as a NLS1 (Berton et al. 2017). The source was detected in the 100 MeV–100 GeV energy range by *Fermi*/LAT (Ackermann et al. 2015).

**4C+15.05** also known as NRAO 91 and PKS 0202+14. On the basis of [O III]  $\lambda 3727$  and [Ne I]  $\lambda 3833$  lines, the source was estimated to be located at  $z = 0.833$  (Stickel et al. 1996), but a smaller redshift of  $z = 0.405$  is reported by Perlman et al. (1998). Recently, Jones et al. (2018) suggested that the neutral hydrogen absorption feature of this source agrees very well with the value of  $z = 0.833$ . The mean spectral index of  $\alpha = -0.33$  between 400 MHz to 8 GHz is reported by (Herbig & Readhead 1992). This source displays a structure of a core and double lobes with a total projected size of  $\sim 1.3$  kpc. A core-jet structure at pc-scale extends the projected size of  $\sim 25$  pc at a position angle perpendicular to the kpc-scale structure (An et al. 2016). Different from 3C 286, the significant apparent superluminal motion of  $\sim 16c$  is detected (An et al. 2016). 4C+15.05 has been identified as a gamma-ray AGN with the EGRET, and later was detected by *Fermi*/LAT.

**4C+39.23B** located at photometric redshift of  $z = 1.18$  (1.0-1.4) (Lilly 1989). The value of  $z = 1.21$  was used in Law-Green (1995) and Roche et al. (1998). The spectral indices between 0.4 to 1.4 GHz and between 4.9 to 8.5 GHz are -0.3 and -1.02, respectively (Fanti et al. 2001). It is detected by *Fermi*/LAT and associated with J0824.9+3916 (Massaro et al. 2016). However, its gamma-ray association is doubtful and could arise from the nearby blazar 4C+39.23 (Migliori et al. 2016; An et al. 2017).

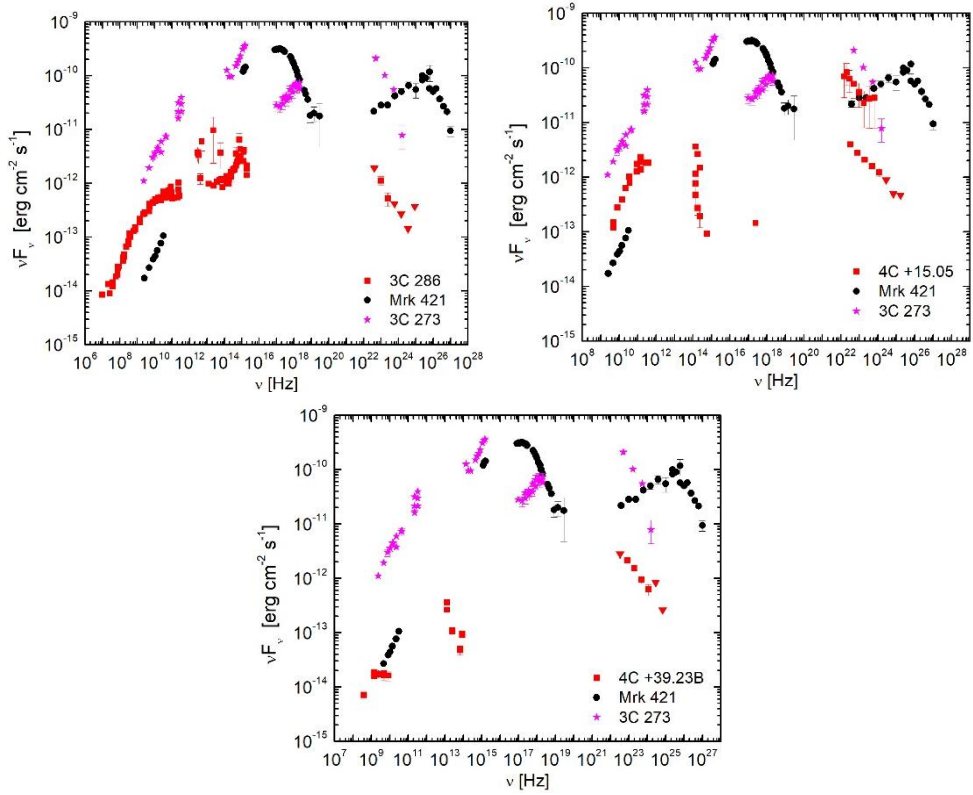


**Fig1.** SEDs of the three gamma-ray emission CSSs. The gamma-ray emission data in the *Fermi*/LAT band for the three CSSs are taken from our work (in preparation). The other data, for 3C 286 are from An et al. (2016) and NED, for 4C+15.05 are from Bloom et al. (1994), Comastri et al. (1997), Sticckel et al. (1996) and Montigny et al. (1995), for 4C 39.23B are from SSDC (<https://tools.ssdc.asi.it/SED/>). The data of two typical blazars, one BL Lac (Mrk 421) and one FSRQ (3C 273), are taken from Zhang et al. (2012, 2014).

### 3. Comparisons of Broadband SEDs between CSSs and Blazars

We collected the data of broadband SEDs for the three CSSs from the literature, as illustrated in Figure 1. The average spectra in the gamma-ray band observed by the *Fermi*/LAT are from our work in preparation. For comparisons, the broadband SEDs of two typical blazars, one BL Lac (Mrk 421) and one FSRQ (3C 273), are also presented in Figure 1. In the radio band, 3C 286 and 4C+15.05 have the higher fluxes than Mrk 421. However, in other energy bands the radiation fluxes of the three CSSs are much lower than that of the two blazars. Especially in the X-ray band, except for 4C+15.05, which has an observational data point in the soft X-ray band, no other observation data are available for the three CSSs, indicating that their X-ray emission is very weak. This is very different from blazars since blazars normally have very strong emission in the X-ray band. The broadband SEDs of the three CSSs, similar to that of blazars, shape two bumps. The peak frequencies of the first bumps for the three CSS SEDs approximately locate at  $10^{12}$ - $10^{13}$  Hz, similar to the typical values of FSRQs. Comparing with the two blazars, the morphology of the broadband SEDs for the three CSSs is more analogous to FSRQs than BL Lacs. The broadband SEDs of blazars are thought to be

dominated by the pc-scale jet radiation. The radiation mechanisms of CSSs in multi-wavelengths are very unclear. The larger viewing angle of CSSs than that of the blazar jets may challenge the one-zone leptonic models to represent the observed SEDs of CSSs.

## References

- [1] Abdo, A. A., Ackermann, M., Ajello, M., et al. 2009, *ApJ*, 699, 31
- [2] Ackermann, M., Ajello, M., Atwood, W. B., et al. 2015, *ApJ*, 810, 14
- [3] Akujor, C. E., & Garrington, S. T. 1995, *A&AS*, 112, 235
- [4] An, T., Cui, Y.-Z., Baan, W. A., Wang, W.-H., & Mohan, P. 2016, *ApJ*, 826, 190
- [5] An, T., Lao, B.-Q., Zhao, W., et al. 2017, *MNRAS*, 466, 952
- [6] Berton, M., Foschini, L., Caccianiga, A., et al. 2017, *Frontiers in Astronomy and Space Sciences*, 4, 8
- [7] Bloom, S. D., Marscher, A. P., Gear, W. K., et al. 1994, *AJ*, 108, 398
- [8] Cohen, A. M., Porcas, R. W., Browne, I. W. A., Daintree, E. J., & Walsh, D. 1977, *MmRAS*, 84,
- [9] Comastri, A., Fossati, G., Ghisellini, G., & Molendi, S. 1997, *ApJ*, 480, 534
- [10] de Vries, W. H., O’Dea, C. P., Baum, S. A., et al. 1997, *ApJS*, 110, 191
- [11] Fanti, C., Pozzi, F., Dallacasa, D., et al. 2001, *A&A*, 369, 380
- [12] Fukazawa, Y., Finke, J., Stawarz, L., et al. 2015, *ApJ*, 798, 74
- [13] Ghisellini, G., Maraschi, L., & Dondi, L. 1996, *A&AS*, 120, 503
- [14] Herbig, T., & Readhead, A. C. S. 1992, *ApJS*, 81, 83
- [15] Jones, K. M., Ghosh, T., & Salter, C. J. 2018, *AJ*, 155, 254
- [16] Law-Green, J. D. B., Leahy, J. P., Alexander, P., et al. 1995, *MNRAS*, 274, 939
- [17] Lilly, S. J. 1989, *ApJ*, 340, 77
- [18] Maraschi, L., Ghisellini, G., & Celotti, A. 1992, *ApJ*, 397, L5
- [19] Massaro, F., Thompson, D. J., & Ferrara, E. C. 2015, *A&A Rev.*, 24, 2
- [20] Migliori, G., Grandi, P., Torresi, E., et al. 2011, *A&A*, 533, A72
- [21] Migliori, G., Siemiginowska, A., Kelly, B. C., et al. 2014, *ApJ*, 780, 165
- [22] O’Dea, C. P. 1998, *PASP*, 110, 493
- [23] Perlman, E. S., Padovani, P., Giommi, P., et al. 1998, *AJ*, 115, 1253
- [24] Roche, N., Eales, S., & Rawlings, S. 1998, *MNRAS*, 297, 405
- [25] Sikora, M., Stawarz, L., Moderski, R., Nalewajko, K., & Madejski, G. M. 2009, *ApJ*, 704, 38
- [26] Spencer, R. E., McDowell, J. C., Charlesworth, M., et al. 1989, *MNRAS*, 240, 657

- [27] Stickel, M., Rieke, G. H., Kuehr, H., & Rieke, M. J. 1996, *ApJ*, 468, 556
- [28] Sun, X.-N., Zhang, J., Lin, D.-B., et al. 2015, *ApJ*, 798, 43
- [29] Tavecchio, F., & Ghisellini, G. 2014, *MNRAS*, 443, 1224
- [30] Urry, C. M., & Padovani, P. 1995, *PASP*, 107, 803
- [31] von Montigny, C., Bertsch, D. L., Chiang, J., et al. 1995, *ApJ*, 440, 525
- [32] Xue, Z.-W., Zhang, J., Cui, W., Liang, E.-W., & Zhang, S.-N. 2017, *Research in Astronomy and Astrophysics*, 17, 090
- [33] Zhang, J., Liang, E.-W., Zhang, S.-N., & Bai, J. M. 2012, *ApJ*, 752, 157
- [34] Zhang, J., Sun, X.-N., Liang, E.-W., et al. 2014, *ApJ*, 788, 104
- [35] Zhang, J., Xue, Z.-W., He, J.-J., Liang, E.-W., & Zhang, S.-N. 2015, *ApJ*, 807, 51